GLATTER, O. (1972). *Acta Phys. Austriaca*, **36**, 307–315.
GLATTER, O. (1979). *J. Appl. Cryst.* **12**, 166–175.
KLOTZ, I. M., LANGERMAN, N. R. & DARNELL, D. W. (1970). *Ann. Rev. Biochem.* **39**, 25–62.
MITTELBACH, P. & POROD, G. (1961*a*). *Acta Phys. Austriaca*, **14**, 185–211.
MITTELBACH, P. & POROD, G. (1961*b*). *Acta Phys. Austriaca*, **14**, 405–439.
MITTELBACH, P. & POROD, G. (1962). *Acta Phys. Austriaca*, **15**, 122–147.
MONACO, H. L., CRAWFORD, J. L. & LIPSCOMB, W. N. (1978). *Proc. Natl Acad. Sci. USA*, **75**, 5276–5280.

Acta Cryst. (1981). A**37**, 382–390

Absolute Thermal Diffuse Scattering Measurements. I

BY JOHN S. REID

Department of Natural Philosophy, The University, Aberdeen AB9 2UE, Scotland

(*Received* 30 *August* 1980; *accepted* 5 *December* 1980)

Abstract

Consideration is given to the quantities required to convert measured X-ray intensities into absolute units for comparison with theoretical predictions. Attention is focused on the instrumental resolution correction and the factors of incident beam spread and wavelength range, crystal mosaic spread, and detector size and efficiency that contribute to the spread of wavevectors necessarily sampled in a given measurement. A scheme is presented for handling each of these factors with confidence and generally without any assumptions as to their simple analytic form. A set of auxiliary measurements is described which enables a practical amount of data to be collected for the required convolutions. The scheme also provides a simple method for aligning the apparatus in a known way. Some numerical examples are given of the effect of the factors on smearing the scattering from KCl in our apparatus.

Introduction

There is a continuing interest in X-ray thermal diffuse scattering (TDS) but the technique of making absolute measurements of TDS cross sections has in the past acquired a reputation for difficulty, one which it does not really deserve. However, it is a technique in which it is of the utmost importance that attention be given to quite a number of details before confidence can be placed in the final results. This importance has been emphasized from time to time by recurring controversy on the accuracy of published experimentally measured phonon scattering intensities. Techniques have changed over the years and therefore, in the interests of discussing points which generally have been neglected in the literature, an account of experimental considerations relevant to obtaining reliable absolute measurements will be presented. A description of our own methods is long overdue because no systematic account has been given, although some aspects have been reported in earlier papers by Buyers & Smith (1966), Pirie & Smith (1968) and Peterson & Smith (1972).

Of course, there is essentially no difference between measuring thermal diffuse scattering and other diffuse scattering caused by disorder or defects, for the scattered photons are not labelled by the scattering process. Hence, the method should be applicable to diffuse scattering in general. However, where theoretical intensities are required, those relevant to thermal scattering will be discussed and numerical values quoted from thermal scattering cross sections. This reflects the limits for which the methods have been tried and tested.

Part I of this account, excepting this introduction, is concerned with recent developments in evaluating the instrumental resolution function, an essential step in the analysis of measurements. Discussion of other aspects of technique is left to part II (Pirie & Reid, 1981) which also presents new absolute measurements for some alkali halides.

Absolute TDS measurements are made on single crystals. The scattering vector **K** is always chosen to be intermediate between reciprocal-lattice points because, apart from using the Mössbauer effect, there is no way of measuring the TDS under Bragg reflections. The only crystal shape in which absorption in an inhomogeneous beam can be handled with complete confidence is a parallel-sided slab where the face presented to the incident beam is large enough to intercept the entire beam. This shape will be assumed, though the procedure that will be described can be extended to handle any sample shape.

Much has been said on the relative merits of photographic recording *versus* direct photon counting

0567-7394/81/030382-09$01.00

but it seems, without going into details here, that, if suitable apparatus is available, there is considerable advantage in using a counter for absolute measurements. This will be assumed in the rest of the discussion, but with appropriate rephrasing the methods are all applicable to photographic detection.

The three main operations which distinguish *absolute* measurements from others are the following:

(1) Relating the observed number of photons s^{-1} scattered into a particular solid angle to a cross section expressed as a fraction of the beam intensity, *i.e.* finding the main beam factor, hereinafter called B.

(2) Changing the above cross section to appropriate theoretical units, usually 'electron units per cell', *i.e.* finding the unit conversion factor, here called E. This involves properties of the sample, including its absorption characteristics, and also factors determined by the geometry of the equipment, its size and the beam polarization.

(3) Making a first-order correction for the instrumental resolution, a correction designated by $(1 + R)$.

When a measurement is made of the scattered intensity, J_{obs}, a value is obtained for the ratio of signal counts to incident beam monitor counts, having subtracted the mean noise in both channels. This measurement is converted to a cross section of I_{obs} in electron units per cell using the equation

$$I_{obs} = J_{obs} \times E/B. \quad (1)$$

In order to produce an experimental cross section I_{exp} appropriate to a single scattering vector $\mathbf{K}$, the smearing effect of the instrument resolution must be corrected by the factor $(1 + R)$. Thus,

$$I_{exp} = J_{obs}(1 + R) \times E/B. \quad (2)$$

Given that the detector is really recording what you want, for example without contamination by harmonic wavelengths, fluorescence or scattering from other than the sample crystal, then accurate conversion to absolute units is assured if the three factors R, E and B are correctly dealt with. Of these, the resolution correction R requires the most discussion and it is to this we turn our attention here.

In the interests of brevity, unity and clarity, reference is not made to other authors' attempts at determining the resolution correction since they tend to suffer from sins of omission and a reliance on analytic representations of the functions involved. No criticism is implied of their results as they pertain to the particular apparatus to which they refer but the author believes that the spirit of the approach described here is more trustworthy. Although the following discussion may seem lengthy, for many pieces of equipment one or more effects may obviously be negligible after an order of magnitude calculation and hence the corresponding section can be omitted.

The resolution correction

Strategy

The incomplete treatment of the resolution correction has been a feature of some past diffuse scattering measurements, it not being uncommon to wish it away altogether without producing evidence that it is small. In fact, it can be quite large and an appreciation of the magnitude of the factors involved is likely to lead to a better use of equipment, even when only relative and not absolute diffuse scattering measurements are being made. Indeed, the situation with diffuse scattering contrasts markedly with that of Bragg scattering, where the resolution function is effectively irrelevant except for considerations introduced by the spread in wavelength of the incident radiation.

It is easy to say that calculating the instrumental resolution function merely involves convolving a few functions together. In practice, collecting enough information for an exact calculation would take a prohibitive amount of time, as would computing the result.

The basic input information required is the complete spatial distribution of the beam intensity at different wavelengths, the three-dimensional mosaic-spread distribution of the sample crystal, and the counter geometry and sensitivity distribution. If the sample crystal is not of the assumed shape, one also needs its complete shape, position and orientation at the chosen scattering configuration. It is doubtful if all these complexities can be handled to the required accuracy and it seems a choice must be made on whether to spend the computing time calculating the effects of an irregular crystal in a uniform beam or the effects of a non-uniform beam with the simple crystal shape assumed. The beam available dictates the choice. In our experience, X-ray beams from bent-crystal monochromaters cannot be represented by uniform functions or even Gaussian functions or other simple analytic expressions. Similarly, mosaic distributions of crystals often do not respect mathematical simplicity. The procedure to be described is based upon a numerical integration using point-by-point measurements of the characteristics of beam, sample and counter. The goal is accuracy and confidence in the resolution with a feasible amount of data collection and computation. The trap is that there is a temptation to cut corners on a lengthy exercise which in the end may produce a correction of only a few percent. Yet one factor inadequately treated may produce a totally spurious result after a lot of work.

The numerical treatment given here has been developed from the approach briefly reported by Buyers & Smith (1966). The resolution correction is intimately linked to the process of aligning and measuring goniometer angles. One by-product of the

approach described here is that it gives a particularly simple and easily reproduceable method of setting the crystal and counter.

With a given setting of goniometer angles, the measured intensity I_{obs} comes from a range of scattering vectors **K** occupying a volume in reciprocal space, irregularly sampled because of non-uniformities of beam, crystal and counter. Any comparison with theoretical intensities $I_{th}(\mathbf{K})$ can only be made after these have similarly been integrated over the same volume in reciprocal space.

Preliminary

It is convenient to have available in reciprocal space three separate (right-handed) sets of reference axes and, of course, algorithms to transform between these axes. With reference to Fig. 1, the following are established:

(*a*) A set of axes {**X,Y,Z**}, the usual axes in which one would express components of the scattering vector as K_x, K_y, K_z, *e.g.* **K** = 1·2, 1·2, 1·2, the units being $2\pi/d$.

(*b*) A set of axes {**A,B,C**}, which essentially defines the scattering plane of interest in the experiment. It is fixed with respect to the crystal structure planes and one would normally expect the crystal to have its incident face perpendicular to the scattering plane. If it has not, then the absorption correction will be more complicated. Let **A** be perpendicular to the crystal face and in the scattering plane, **B** lie parallel to the crystal face and in the scattering plane, and **C** lie parallel to the crystal face and perpendicular to the scattering plane. Thus, a crystal suitable for reflection measurements of the above wave vector might have **A** = [110], **B** = [001] and **C** = [1$\bar{1}$0] in terms of {**X,Y,Z**}.

(*c*) A set of axes {**R,S,T**}, which define convenient axes to generate a uniform mesh of points in reciprocal space at which theoretical intensities can be calculated, *e.g.* **R** = [111], **S** = [11$\bar{2}$], **T** = [1$\bar{1}$0] in terms of {**X,Y,Z**}. Usually **T** is parallel to **C** but the origin of the {**R,S,T**} axes is not the origin of reciprocal space.

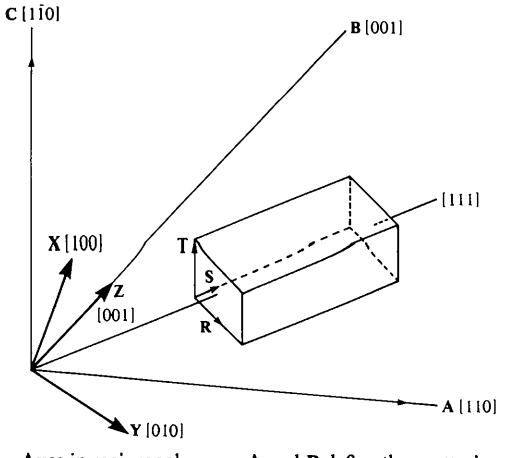

Fig. 1. Axes in reciprocal space. **A** and **B** define the scattering plane (a specific example is shown) which contains a direction [111] along which the scattering is to be investigated. **R**, **S**, **T** and associated steps define a mesh of points at which the theoretical scattering can be calculated.

Alignment

It is assumed that the X-ray beam has been aligned more or less perpendicular to the common axis of rotation of crystal and counter (ω and θ axes). The following steps refer to collecting the data necessary for calculating the resolution function. Fig. 2 shows the components to which reference will be made.

It is possible to obtain information on the spread of the beam perpendicular to the scattering plane by scanning a pair of slits. However, it is simpler to arrange on a scanning platform in front of the counter a converging Soller slit which will provide the exact information relevant to convolving in the direction perpendicular to the scattering plane. Only one scan of this slit is made and the profile $S(J)$ against the corresponding micrometer reading (J) is recorded for use in the convolution. As to the specification of this Soller slit, see the section on *Perpendicular beam spread.*

With the Soller slit removed, the beam distribution in the scattering plane is now mapped with the aid of a pair of fine slits, P and Q, positioned as far apart as possible as shown in Fig. 2. This distance in our equipment is 290 mm. These fine slits must be rigidly mounted perpendicular to the scattering plane and must be sufficiently long to allow the whole vertical distribution of the beam to pass. They should be accurately relocatable and must stay parallel while being tracked.

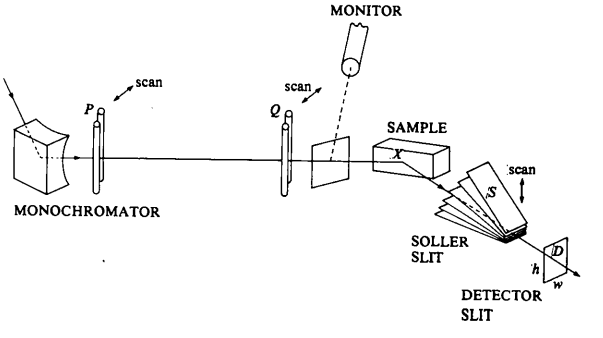

Fig. 2. The essential experimental components relevant to the collection of data for calculating the resolution function. The fine slits P and Q are perpendicular to the scattering plane and are scanned in the scattering plane. The converging Soller slit S is scanned perpendicular to the scattering plane. P, Q and S are all removed before making a diffuse scattering measurement but permanent beam limiting slits, which are not shown in the figure, remain. The incident beam strikes the sample crystal at X whose position along the sample depends on the selected position of P and Q. h and w are the height and width of the detector slit D as measured perpendicular and parallel to the scattering plane respectively.

The required performance can be checked optically. We use dowels to locate the slit holders and accurately machined dovetailed slides for the movement, but a kinematic mount and slide would be better. If the whole beam is measured, the slit widths must be as wide as the step between successive settings. If the beam is sampled only, narrower slits can be used.

A good analysing crystal of LiF, calcite, or any material with a mosaic sufficiently narrow to separate clearly the α_1 and α_2 reflections on an accessible Bragg peak is obtained and put into the sample holder. For each pair of fine slit settings the crystal is rocked through the α_1 and α_2 reflections and the intensity of these recorded. The fine slits are moved systematically across the whole beam enabling one to build up a table of the beam structure containing typically a few hundred intensity entries. The step chosen depends on the irregularity of the beam. This basic data need be collected only once for a given beam but should be collected at the normal voltage and current settings for the tube. The validity of this data for analysis lies in the assumption that in planes parallel to the mean scattering plane, the overall beam intensity may be different but the relative distribution within the plane does not change much, at least in the region where the bulk of the intensity lies. Hence, sampling the distribution by perpendicular slits is a reasonable procedure.

One particular pair of fine slit settings is selected at or near the mean of the beam and the fine beam let through by these slits is designated the reference beam. Subsequent setting up of the goniometer for a required scattering vector uses this reference beam so that it is known with certainty which part of the beam has the required **K** coordinates in the scattering plane. If quite wide slits have been used to map the beam, it may be advisable to use finer slits to define the reference beam to within about 1′ arc.

After replacing the analysing crystal by the sample crystal, a simple ω scan is performed with the reference beam, or any other fine beam, to give a measure of the mosaic spread distribution, which will be needed in the convolution. This must be checked for uniformity across the region of the crystal which will be sampled by the spread of the incident beam incurred by the range of scattering angles to be used. Also, the scan should be repeated for several different rotations about an axis perpendicular to the crystal face to give some idea of the isotropy or otherwise of the mosaic distribution.

Temporarily restricting the beam to a small square cross section at the counter and using an absorbing foil if necessary, a fine pencil beam can be scanned directly over the useful region of the signal counter to build up a map of its relative efficiency. This may also be used in the convolution, but our experience suggests that a new scintillation counter, for example, is likely to be uniform to within 1% over a sizeable proportion of its surface. Nevertheless, scintillators deteriorate and this uniformity is worth checking from time to time. Si(Li) detectors also appear to be uniform.

All the information required for the numerical convolutions is now at hand. The goniometer is carefully aligned, with the rotation axis passing through the reference beam. The sample crystal is centred, strictly speaking with the rotation axis passing through the mean scattering point (as will be discussed in part II). With the fine reference beam and then the Soller slit, an iterative procedure of successively rotating the crystal about the A and C axes quickly secures alignment on a Bragg peak with reciprocal-lattice vector near the region of reciprocal space of interest. It is important to record which points on the mosaic-spread curve and on the Soller-slit profile curve (preferably the mean) are used for setting up because these provide the respective zeros about which the convolution is carried out. It is also necessary to record whether Ka_1, Ka_2 or a certain mean wavelength is used in the alignment and change of angles.

The correction R

With the alignment procedure just sketched, once the goniometer has been adjusted for a particular value of scattering vector **K** in the scattering plane of interest, it is those rays of the reference beam which pass through the Soller slit at its set position and arrive at the mid-point of the counter area which have exactly the chosen scattering vector **K**. All other scattering intensity recorded at different parts of the receiving area, or from different incident rays, have different scattering vectors. However, information has been collected to enable one to determine exactly how the surrounding region of reciprocal space is sampled.

The theoretical scattering intensity $I_{\rm th}(\mathbf{K})$ is calculated at **K** and numerically convoluted in the region surrounding **K** using the data collected. This convolution results in a value $I^c_{\rm th}(\mathbf{K})$. The resolution correction is determined by the change which the convolution produces, namely,

$$R' = \frac{I_{\rm th}(\mathbf{K}) - I^c_{\rm th}(\mathbf{K})}{I^c_{\rm th}(\mathbf{K})}. \qquad (3)$$

Strictly speaking, a comparison between an experimental value of $I_{\rm obs}(\mathbf{K})$ and theoretical value of $I_{\rm th}(\mathbf{K})$ should be made by comparing $I_{\rm obs}(\mathbf{K})$ with $I_{\rm th}(\mathbf{K})/(1 + R')$.

However, this comparison is not entirely satisfactory because $I_{\rm th}(\mathbf{K})/(1 + R')$ contains a mixture of theoretical and apparatus-dependent terms. In practice, it is better to compare $I_{\rm th}(\mathbf{K})$, a property independent of the apparatus, with its experimental equivalent $I_{\rm exp}(\mathbf{K}) = (1 + R) I_{\rm obs}(\mathbf{K})$, hence the use of (2). The correct R to use in this equation is determined by a convolution of the true intensity distribution in reciprocal space,

requiring for its precise determination an iterative procedure and a great many measurements. In practice, (2) is indeed used but with

$$R = R', \tag{4}$$

the justification for convolving the theoretical intensities rather than the true ones being that the difference between the two varies slowly in reciprocal space compared with the rapidity of variations which significantly affect R.

The convolutions

Once it is accepted that resolution corrections can be confidently made, it is worth considering the design of apparatus to the limit of this confidence. For this reason, and to provide a clear idea of how reciprocal space is sampled in different ways by different effects, the following sections give some detail of the smearing produced by beam, mosaic and receiving area. In truth, there are not many pieces of apparatus dedicated specifically to measuring TDS but there are a great many X-ray scattering installations to which similar considerations apply, although the details are not always appreciated. For instance, an extremely narrow beam scattered by a perfect crystal may produce Bragg reflections of a few seconds of arc width but may at the same time receive diffuse scattering from a very appreciable region in reciprocal space around the Bragg reflection. In a different situation, a photographic plate may effectively be considered as a surface of independent point receivers and yet at each point there will be an intensity which is the integral of the diffuse scattering over an odd-shaped, and possibly quite sizeable, region of reciprocal space.

Detector slit effects

Fig. 3 illustrates how the spread of scattered wavevectors ($\mathbf{k}_1$) allowed by a finite slit samples an area of reciprocal space, or, more strictly, a volume whose thickness is determined by the wavelength spread $\Delta\lambda$. The use of a circular slit poses an unnecessary complexity in the numerical integration. It also removes the possibility of making use of the greater tolerance which usually exists to spread perpendicular to the scattering plane compared to spread within the scattering plane.

Since we have so far been able to use counters with a uniform response, we have not needed an efficiency function to weight different parts of the sampled area. The total area is not significantly different for α_1 and α_2 wavelengths and hence a mean wavelength appropriate to the beam may be used. Centring on each point of the **RST** mesh and interpolating in between as described later, the theoretical intensity is convolved with a uniform function of constant size and orientation representing the slit height.

As for the slit width, some time may be saved with its convolution if this is not performed first but made the penultimate convolution before taking account of the individual α_1 and α_2 beam distributions within the scattering plane. The theoretical intensities need be convolved at this stage only at the subset of points within the scattering plane. However, the change in angle of the sampled line of points with changing angle of $\mathbf{k}_1$ must be incorporated.

Mosaic spread effects

The sampling of reciprocal space introduced by the mosaic distribution is illustrated in Fig. 4. The spread increases directly with the magnitude of **K**. The figure shows clearly that it is not just the mosaic as measured by rotations of the sample perpendicular to the scattering plane which is relevant but in general the whole three-dimensional distribution of mosaic. This data is scarcely accessible in most circumstances and there is little alternative to assuming an isotropic distribution with a shape given by some average of experimental determinations. Fortunately, for a reasonably good crystal the spread in reciprocal space introduced by the mosaic is typically the smallest of all the factors involved. Unfortunately, it requires the greatest effort to calculate. Reducing the spherical cap to a circular area does not significantly help and neither does introducing an analytic function for the mosaic. In the absence of any obvious simplification which would not at the same time introduce uncertainty, our theoretical intensities are convoluted numerically over the spherical cap, as required.

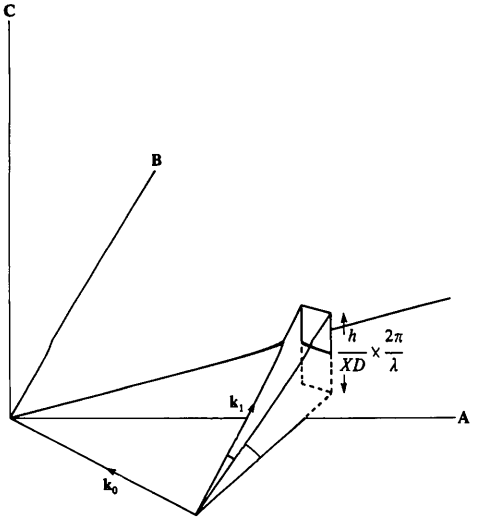

Fig. 3. Illustration of the detector slit smearing in reciprocal space. The detector slit of dimensions h, w at crystal–slit distance XD (see Fig. 2) allows a range of scattered wavevectors $\mathbf{k}_1$ to sample an effectively planar area, as shown for one incident wavevector $\mathbf{k}_0$. (The scattering vector $\mathbf{K} = \mathbf{k}_1 - \mathbf{k}_0$.)

Details of this convolution, or any other, are not spelt out here for they would merely clothe the line of development in routine geometrical complexity.

Perpendicular beam spread

Fig. 5 shows exactly how the beam spread perpendicular to the scattering plane involves sampling reciprocal space with non-zero $\mathbf{K}_c$ components.

What might appear at first sight a lengthy problem involving the complete crossfire details of the vertical beam distribution yields to a very simple solution by allowing three approximations involving little loss of accuracy. These assumptions are: (1) upon rotation of the crystal, the interception height v of a ray does not change significantly; (2) in any apparatus suitable for diffuse scattering measurements, the fractional change in the distance XD is small and, indeed, for this convolution, XD can be taken as the distance between rotation axis and detector for all beams; (3) at least in the region containing most of the beam intensity, the perpendicular beam distribution does not change rapidly with the plane selected to measure this distribution. Operationally, the validity of this approximation can be checked by using the P, Q slits to select different perpendicular planes whose distribution can be scanned by the Soller slit described in the next paragraph.

The convoluting function for the perpendicular beam spread is that distribution which samples all incident beams of constant $(\varphi - v/XD)$. Fig. 6, with the accompanying legend, shows that a converging Soller

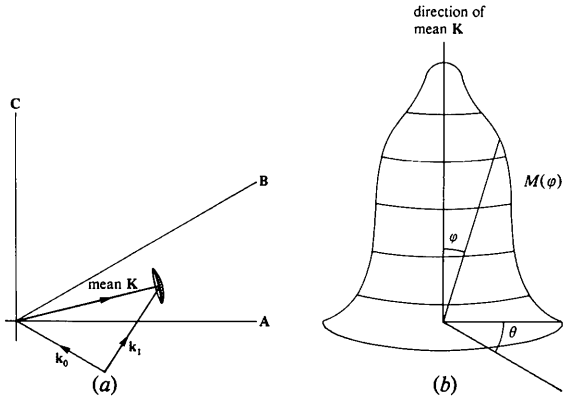

Fig. 4. Illustration of the mosaic-spread smearing in reciprocal space. (*a*) For a given incident wavevector $\mathbf{k}_0$ and scattered wavevector $\mathbf{k}_1$, the mosaic distribution causes reciprocal space to be sampled over a surface in the form of a spherical cap about the end of the mean scattering vector $\mathbf{K}$. (*b*) In spherical polar coordinates (r,θ,φ) with mean $\mathbf{K}$ as the z axis, the spherical cap is sampled by the mosaic function $M(\theta,\varphi)$ which could, in principle, also depend on the direction of $\mathbf{K}$. In practice, an average isotropic distribution $M(\varphi)$ is likely to be an adequate approximation in almost all cases.

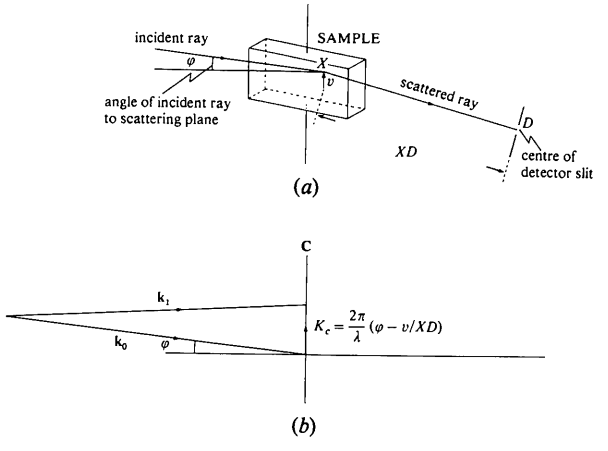

Fig. 5. Illustration of the component of the scattering vector perpendicular to the scattering plane caused by a skew ray. (*a*) In real space an incident ray striking the sample crystal at point X at an angle φ to the scattering plane and at a distance v from the scattering plane. (*b*) In reciprocal space the resulting component of the scattering vector perpendicular to the scattering plane is $K_c = 2\pi(\varphi - v/XD)/\lambda$.

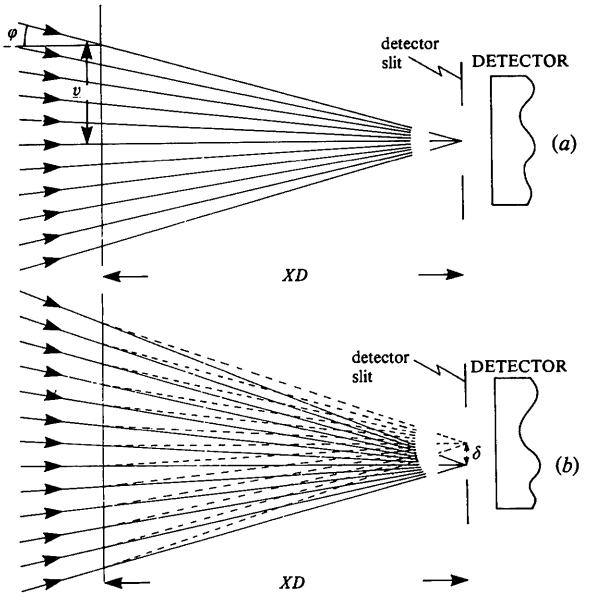

Fig. 6. Illustration of how the set of beams with constant K_c are sampled by a converging Soller slit. The figure shows a section of real space perpendicular to the scattering plane with distances in this direction (such as v) exaggerated relative to those in the scattering plane (such as XD). (*a*) All the incident beams on the left will reach the mid-point of the detector after scattering with zero component of scattering vector perpendicular to the scattering plane (*i.e.* $K_c = 0$). A converging Soller slit centred on the detector (slit), as sketched in Fig. 2, with a narrow spacing between the plates will allow the total intensity of these beams to be measured. (*b*) When the Soller slit is scanned down a distance δ, the intensity received by the detector corresponds to a different set of incident rays. All these rays when scattered to the mid-point of the detector slit undergo scattering with the same perpendicular component of scattering vectors, namely $K_c = (2\pi/\lambda)(\delta/XD)$.

slit centred on the detector slit will enable this distribution to be found experimentally by a single scan.

The converging Soller-slit technique only works for the distribution perpendicular to the scattering plane because the mean value of K_c is approximately zero for all scattering angles. It is generally impractical to use the method to map the spread within the scattering plane because two scans would be needed with changing scattering angle. However, under special circumstances this might be an advantageous procedure over an exhaustive P, Q slit mapping.

In passing, it is worth noticing that in the plane perpendicular to the scattering plane the spread sampled in reciprocal space is a minimum when the doubly-bent monochromator crystal focuses the beam at the detector slit and not at the sample. Buyers constructed such a monochromator for our apparatus in 1963.

Scattering plane beam spread

When allowance is made for the different positions at which the different beams selected by the P, Q slits strike the sample, no two beams scattered to the mid-point of the counter are associated with the same scattering vector. Fig. 7 shows how the variation in incident and take-off angles causes a spread in reciprocal space, and a later section will show in detail the range of **K** values that may be covered. This is the final convolution performed and need only be carried out for **K** values of interest within the scattering plane.

Theoretical intensities

Requirements

Equations (3) and (4) show that the resolution correction depends on the effect of the convolution, namely $(I_{\text{th}} - I_{\text{th}}^c)$. It is clear that if I is increased by a constant then this effect remains unchanged. It is also easy to show that if the convoluting function is centred about its mean point then a linear variation of I with **K** makes no difference to I_{th}^c. Hence, under normal circumstances it is the curvature of the intensity variation which determines R' and hence R. Therefore, one should only obtain appreciable values of R where the curvature of the total scattering cross section is appreciable. When this happens in practice, most of the curvature resides in the 1-phonon scattering (I_1). The other contributions to the scattering such as the sum of the multiphonon and anharmonic scattering (I_n), and the Compton scattering (I_{Compt}) are either relatively small or, in regions where they are comparable or even larger than I_1, they can reasonably be taken to vary linearly over the volume sampled by a particular scattering beam geometry. Hence, writing

$$I = I_1 + I_n + I_{\text{Compt}}, \tag{5}$$

let

$$R_1' = \frac{I_1 - I_1^c}{I_1^c}, \tag{6}$$

then

$$R' = R_1' \frac{I_1^c}{I_1^c + I_n + I_{\text{Compt}}} = \frac{R_1'}{1 + (1 + R_1')(I_n + I_{\text{Compt}})/I_1}. \tag{7}$$

Therefore, only the 1-phonon scattering need be convolved to give I_1^c and, through (6), (7), (4) and (2) the required correction to the observed intensities. This is a most useful simplification.

Although it is easy to align the apparatus with reference to the mean mosaic position, the mean Soller-slit setting and the centre of the counter, for the

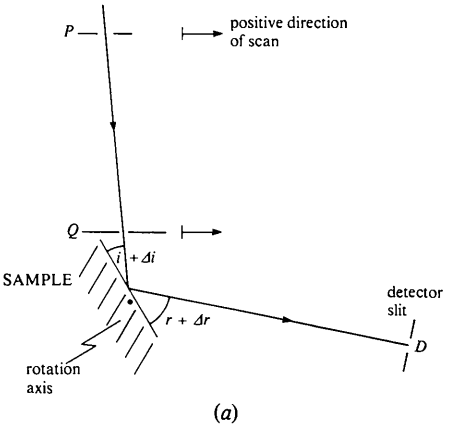

(*a*)

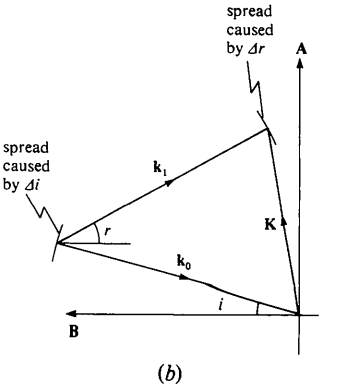

(*b*)

Fig. 7. Illustration of the sampling of reciprocal space within the scattering plane by the main beam. (*a*) In real space a sub-beam defined by the fine slits P and Q moved away from the reference beam settings by amounts ΔP and ΔQ respectively. (*b*) The spread in reciprocal space caused by $2\pi\Delta i/\lambda$ and $2\pi\Delta r/\lambda$. In magnitude $\Delta i = (\Delta Q - \Delta P)/PQ$ and $\Delta r = (\sin r/\sin i)\,(QX\Delta P - PQ\Delta Q)/XD.PQ$, where PQ represents the distance between components P and Q, and similarly for other distances.

above simplification to be most effective the reference beam must not be arbitrarily chosen but must be the mean of the whole beam. It is easy to test whether the chosen beam is adequately near to the mean by calculating R_1' for a test linear function of $I_1(\mathbf{K})$.

Interpolation and integration

The 1-phonon scattering intensities must be generated over a volume mesh of points covering the sampled region and defined by axes {**R**,**S**,**T**} and the associated step widths. A satisfactory but not over-generous density for the mesh gives 20 steps from zone centre along [001] to the zone boundary. A non-linear interpolation is clearly essential and the simplest approach works well. A second-order Taylor expansion is made about the nearest mesh point using 16 first- and second-neighbour values, and the mesh point value, to estimate the nine derivatives involved (in three dimensions). Since second derivatives cannot be estimated accurately at the edge of the mesh, the volume should be chosen sufficiently large that the region sampled by the apparatus does not come to the edge.

Each convolution is performed on the intensity function generated by the previous convolution. Since the process is non-linear, the total effect cannot be found by summing the individual effects of each term acting on its own on the raw theoretical intensities. The integrations are made using Simpson's rule. Since this rule accurately integrates a cubic, there is a simplification possible if the Taylor expansion is always centred on the mesh point whose convoluted intensity is being found, rather than on the nearest mesh point to the **K** value reached in the integral. This simplification produces a less accurate representation of the intensity at some distance from a mesh point but avoids numerical problems that can arise because the approximation produced by moving the expansion point is not everywhere smooth, though it is locally more accurate. Both methods are easy to implement and the only way to judge whether the simplification gives a useful saving in time with negligible or acceptable introduction of error is to make a numerical comparison in some expected 'worse cases'.

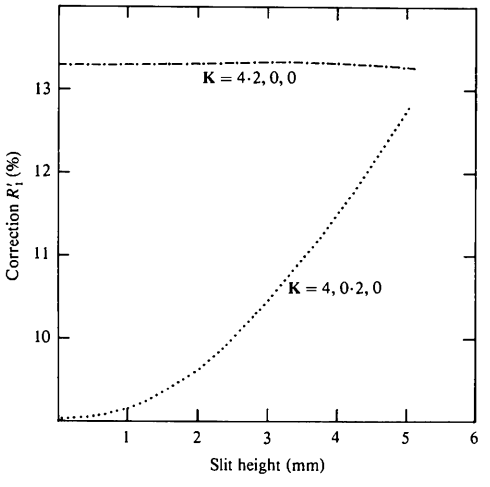

Fig. 8. Examples of the variation of the correction term R_1' with slit height. Two **K** values in the (001) scattering plane illustrate the range of behaviour. The reason for the difference in the two cases can be understood by examining the 1-phonon contours in the region of 400 which are similar to the contours around 600 shown in Fig. 11. The slit is at a distance of about 340 mm from the sample.

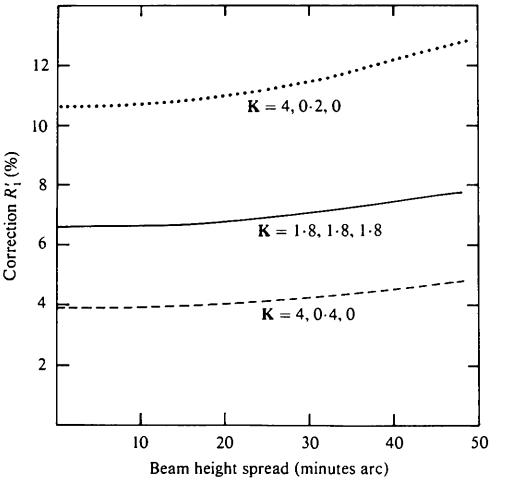

Fig. 9. Examples of the variation of the correction term R_1' with vertical beam profile width. The contribution to the correction from this effect is generally acceptable with a full beam spread of up to 1° perpendicular to the scattering plane.

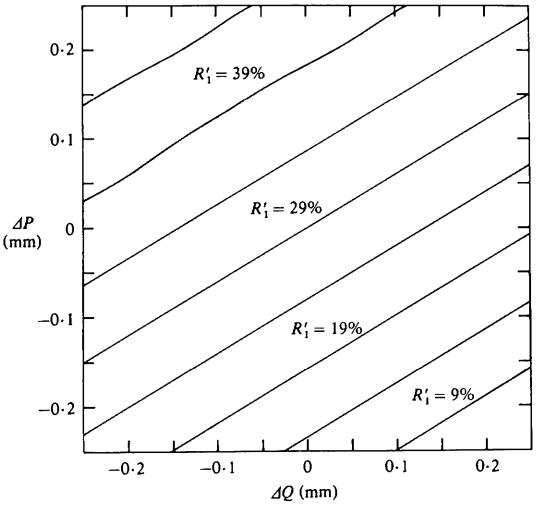

Fig. 10. Example of the variation of R_1' with selected reference-beam position. The chosen scattering vector **K** = 1·9, 1·9, 1·9 in the (1$\bar{1}$0) scattering plane illustrates that R_1' can be quite sensitive to the selected reference beam. Moving either slit by 0·1 mm is equivalent to an angular change in the selected incident ray of about 1·2′ arc. As explained in the text, the reference beam should not be chosen to give zero R_1' but should be chosen to give zero effect with a linear scattering function.

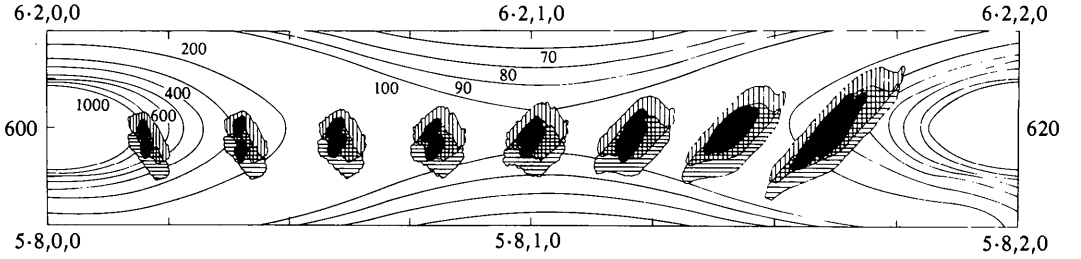

Fig. 11. Illustration to show that the shape and size of the sampled area in the scattering plane can depend on the scattering vector **K**. The reference beam is set to selected points with scattering vector $6,K_y,0$. The diagram shows a section of the (001) scattering plane with 1-phonon intensity contours in electron units per cell for KCl. Around each point the vertically hatched area represents the region sampled by the $K\alpha_1$ beam, with the enclosed black area indicating where 90% of the intensity lies. The horizontally hatched area similarly represents the region sampled by the $K\alpha_2$ beam (which is itself about half the strength of the $K\alpha_1$ beam). The changing area effect is exaggerated here because as $\mathbf{K} = 620$ is approached the incident beam makes a very shallow angle of incidence with the crystal surface. However, it is always present to some extent and originates from the effect described in Fig. 7. The same cause explains why the two different reflection geometries giving the same **K** value have associated with them different correction terms.

Behaviour of the individual contributions

The whole exercise of evaluating the resolution function with some accuracy has two main aims. The first is to set up a numerical simulation of the effect of all the important experimental parameters, allowing trials to be made of the effect of varying these parameters. These trials show trends and values not confused by the uncertainty of counting statistics, which seriously hinder the corresponding real trials, supposing them to be possible. They also produce the answers relatively quickly, allowing, for example, some optimization of design by matching the resolution produced by different effects. One cannot be certain, however, that the model of the complete system of apparatus and scattering function is accurate (for if one could there would be no point in making the experiment) and hence some real trials must also be undertaken. Nevertheless, the exercise is valuable because some parameters, such as the sample 'mosaic spread', cannot be varied easily. The second aim of the exercise is, of course, to provide the best possible corrections for interpreting experimental results.

Figs. 8–11 show some effects of varying the parameters of our apparatus with KCl as a scatterer. The results cannot be said to be 'typical' because there is no standardization of apparatus suitable for diffuse scattering studies. The exact values of R'_1 depend on the size and geometry of the apparatus, all the details of which would cloud the issue. In fact, to illustrate the effects clearly with large absolute changes, points have been chosen closer to Bragg peaks than this particular apparatus was designed to operate customarily. Normally, one effect would not contribute more than a few percent, and probably much less, making it difficult to check the prediction experimentally. The diffuse scattering is generally sufficiently weak that it is not possible to restrict further slit or beam sizes and yet collect sufficient data with a small enough statistical spread to reveal a trend accurately.

The uncertainty in the calculated result depends on the statistical uncertainty in the governing data collected (particularly the beam sampling), the validity of approximations used in the treatment and the realism of the intensity function convolved. The uncertainty in the data collected can be reduced to quite small proportions. The approximations involved are not only normally applicable but can be checked experimentally or numerically, as has been suggested at appropriate places in the text. Ultimately, the confidence in the correction stems from the feeling that all the ingredients have been properly treated.

The resulting corrected experimental measurements (equation 2) will give a figure for comparison with the theoretical intensities which represents a measure of agreement, or disagreement, not at one scattering vector **K** but over a surrounding volume in reciprocal space. In general, a true deconvolution of the experimental results requires more measurements over a small volume in reciprocal space than is usually practicable, followed by an iterative application of the resolution correction. In practice, however, unless the scattering at the **K** value of interest reflects some highly localized singular value, the method described provides an effective deconvolution. It is an equally valuable assurance of confidence in measured intensities if the method unequivocally shows that no resolution correction is required.

The author would particularly like to thank Dr J. D. Pirie for many helpful discussions on the topics discussed here.

References

BUYERS, W. J. L. & SMITH, T. (1966). *Phys. Rev.* **150**, 758–765.
PETERSON, G. C. & SMITH, T. (1972). *J. Phys. F*, **2**, 7–18.
PIRIE, J. D. & REID, J. S. (1981). In preparation.
PIRIE, J. D. & SMITH, T. (1968). *J. Phys. C*, **1**, 648–657.